

Analysis of tapered composite structures using a refined beam theory

Original

Analysis of tapered composite structures using a refined beam theory / Zappino, E.; Viglietti, A.; Carrera, E.. - In: COMPOSITE STRUCTURES. - ISSN 0263-8223. - 183:(2018), pp. 42-52. [10.1016/j.compstruct.2017.01.009]

Availability:

This version is available at: 11583/2692894 since: 2017-11-20T17:33:15Z

Publisher:

Elsevier Ltd

Published

DOI:10.1016/j.compstruct.2017.01.009

Terms of use:

This article is made available under terms and conditions as specified in the corresponding bibliographic description in the repository

Publisher copyright

Elsevier postprint/Author's Accepted Manuscript

© 2018. This manuscript version is made available under the CC-BY-NC-ND 4.0 license
<http://creativecommons.org/licenses/by-nc-nd/4.0/>. The final authenticated version is available online at:
<http://dx.doi.org/10.1016/j.compstruct.2017.01.009>

(Article begins on next page)

Analysis of tapered composite structures using a refined beam theory.

E. Zappino*, A. Viglietti[†] and E. Carrera[‡]

*Mul² Team, DIMEAS, Politecnico di Torino
Corso Duca degli Abruzzi 24, 10129 Torino, Italy.*

Abstract

This work presents some static analyses on reinforced thin-walled tapered structures made of composite material. These applications are performed through a refined one-dimensional model based on the Carrera Unified Formulation. This formulation uses polynomial expansions to describe the displacement field over the cross-section of the beam. In this way, a quasi three-dimensional solution can be obtained. In the present work the cross-sectional kinematic has been described using the Lagrange polynomials. The use of such models allows any component of the structure to be modelled separately and then the complex structure can be obtained thanks to the so-called component-wise approach. Different aeronautical structural components, gradually more complex, have been studied. The stress and displacement fields due to simple loads have been obtained. The results have been compared with those obtained by means of a commercial FEM tools using one-, two- and three-dimensional elements. The results obtained show how the present approach can deal with complex structures such as tapered aeronautical components. The use of refined beam models allows complex stress fields to be accurately evaluated that is composite materials can be investigated.

Key words: CUF, One-dimensional model, tapered beam, composite material, laminate.

*Assistant Professor, Department of Mechanical and Aerospace Engineering, enrico.zappino@polito.it

[†]Ph.D. Student, Department of Mechanical and Aerospace Engineering, andrea.viglietti@polito.it

[‡]Professor, Department of Mechanical and Aerospace Engineering, erasmo.carrera@polito.it

1 Introduction

The tapered thin-walled structures (TWSs) are widely used in the aeronautical field due to their high performances (in mass/stiffness ratio terms) when bending and torsional loads are applied. Several similar examples can be found in the automotive or civil structures. Aeronautical structures have often a slender thin-walled geometry and in many cases, such as in the wing structures, they are also tapered. Therefore the geometrical and structural proprieties change along the structure length, for example, the moment of inertia can be not constant.

For this reason the classical Euler-Bernoulli beam theory [1] can be used considering the stiffness coefficients as a function of the beam axis coordinate. The typical example is a tapered beam where the section changes along the beam axis. In this case, if the beam axis is coincident with the y -axis, the term EI (the bending stiffness) can be written as $EI(y)$ where the moment of inertia, $I(y)$, is variable in function of y . If the material changes along the beam, the elastic modulus E becomes a function of y too. This approach can be found in different works, such as the work by Banerjee and Williams [2]. Cicala [3] and Timoshenko and Goodier [4] proposed different analytical methods. To face the tapered beam structure problem these also include the shear stress in the tapered beam analysis.

A classical approach to the analysis of tapered structures involves the subdivision of the structure into several rigidly joined prismatic beams, each of those with a different cross-section. In this way, maintaining the same classical beam theory, an approximate behavior of a tapered shape can be achieved. In this way the use of classical beam models can be extended to the analysis of beams with a variable section. An example of this approach, named *stepped of piece-wise approach*, can be found in work by Ji Yao Shen *et al.* [5]. This method can show some limits in the case of members with a significant tapered edge; They should be divided into several subsections to obtain accurate results.

After the introduction of the matrix methods by Arigyris and Kesley [6] and the Finite Element Methods (FEMs) by Turner *et al.* [7], many new approaches for the analysis of tapered structures have been presented. In 1977 Just [8] proposed a modified stiffness matrix for tapered components. His work takes into account the variations of the cross-section properties along the beam axis using a proper modified displacements function. In 1978, Schreyer [9] included the generalized Kirchhoff hypothesis and the evaluation of the traverse shear strain for tapered beams. Brown [10] introduced a new stiffness matrix formulation to describe linearly tapered beams. In the civil engineering field, Tena-Colunga [11] has recently provided a practical method based on the Eulero-Bernulli theory to define 2D and 3D elastic stiffness matrices for tapered and curved elements.

In the design of aeronautical project, the TWSs are the most used due to their capability to undergo the aerodynamic loads providing a light structure. Bruhn

[12] discussed classical methods to achieve an approximate solution of aeronautical structure analyses. Recently, these methods have been analyzed by Carrera [13]. In 1961, Benscoter [14] and Vlasov [15] introduced warping functions in order to provide the capability to study TWS using beam models. In the following years, several beam theories able to deal with thin-walled structures have been proposed. In 1986, Waldron [16] proposed the sectoral method. Considering the general beam theory, this approach includes the warping restraint effects when a non-uniform torsion is applied. Recently, many works based on the Variational Asymptotic Method (VAM), dealing with tapered beams, have been presented by Yu and his research group [17–19]. Kim and Kim [20] and Shin *et al.* [21] have recently introduced a higher order beam theory which also works with tapered beams, based on the Vlasov theory.

Carrera presented an advanced numerical tool, called the Unified Carrera Formulation (CUF) [22]. This formulation allows refined structural models to be derived in a compact form. Talking about one-dimensional models, Carrera *et al.* [23] presented a refined beam model where the cross-sectional displacements are approximated using general expansions. In this work the Taylor polynomials are used as expansions. Carrera and Petrolo [24] used Lagrange polynomials to derive a refined beam model with only displacements as the unknowns. Other several classes of models which use different expansions have been proposed in the following years. More details about the CUF can be found in the book by Carrera *et al.* [25].

Carrera *et al.* [26,27] extended the use of CUF to the analysis of complex structures using the *Component-wise approach* (CW), which allows each component of a structure to be represented with a different beam element. Carrera and Zapino [28] extended the use of refined one-dimensional models to complex structures arbitrarily oriented in the space. In the last 50 years, the introduction of composite materials has had a fundamental importance to increase the weight saving in the TWSs. The introduction of these materials requires the use of complex models which are able to describe the complex stress field

In the framework of the CUF, the composite materials have been taken into account since the first work of Carrera [29] and he continued the study in several works such as [30] [31]. More recently improvements of the CUF on the study of the composite material have been performed by [32] [33] [34] [35] where different function have been implemented to obtain displacement fields that increase the reduction of the computational cost without affecting the accuracy.

This work extend the use of these refined 1-D models to the analyses of tapered structures made of composite materials. At first, some assessment results of a no-tapered structure is presented to verify the extension to the composite material. After that, different tapered structures are presented. In these analyses

the displacement field and the stress field are investigated.

2 Refined one-dimensional models formulation

In this section, an overview of the mathematical approach used in this work is introduced. The first part concerns the explanation of the basis to define the displacement, stress and strain fields. After that, the Carrera Unified Formulation for 1-D models is presented followed by the FEM solution which is used to solve the problem. Finally the approach used to study tapered beams is introduced.

Preliminaries

In this work two types of coordinate frames can be individuated. The first frame (x_G, y_G, z_G) is the global reference system used to describe the geometry of the whole structure. The second frame (x, y, z) is related to the local beam formulation and it is used to describe a structure at the element level. y is the local beam axis. x, z represent the plane of the beam cross-section. These frames are figured in Figure 1.

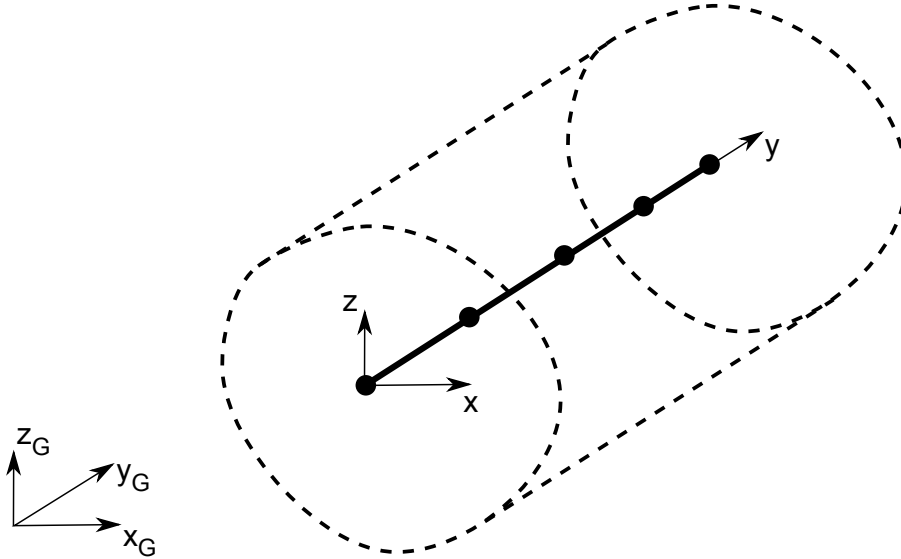


Figure 1: Reference system representation.

The local displacement field \mathbf{u} at each point can be defined as:

$$\mathbf{u}^T(x, y, z) = \{u_x \ u_y \ u_z\} \quad (1)$$

where the three terms are the displacement values along the three axes x, y and z . The stress vector $\boldsymbol{\sigma}$ and the strain $\boldsymbol{\epsilon}$ can be written as follows:

$$\boldsymbol{\sigma}^T(x, y, z) = \{\sigma_{xx}, \sigma_{yy}, \sigma_{zz}, \tau_{xy}, \tau_{xz}, \tau_{yz}\} \quad (2)$$

$$\boldsymbol{\epsilon}^T(x, y, z) = \{\epsilon_{xx}, \epsilon_{yy}, \epsilon_{zz}, \epsilon_{xy}, \epsilon_{xz}, \epsilon_{yz}\} \quad (3)$$

To define the geometrical relations the differential operator \mathbf{b} (a 6×3 matrix) is introduced to obtain the following linear strain-displacement relation:

$$\boldsymbol{\epsilon} = \mathbf{b}\mathbf{u} \quad (4)$$

The explicit formulation can be found in the book by Carrera *et al.* [25].

The stress field is derived using the linear form of the Hook's law; in compact form it can be written as:

$$\boldsymbol{\sigma} = \mathbf{C}\boldsymbol{\epsilon} \quad (5)$$

where \mathbf{C} is the 6×6 *material stiffness matrix*. It contains the elastic coefficients and it is referred to a material reference system (1, 2, 3). The material properties can be arbitrarily rotated of an angle θ around the axis 1 that correspond with the z -direction. When $\theta = 0$ the longitudinal direction of the material corresponds with the beam axis. The problem is represented in fig.2.

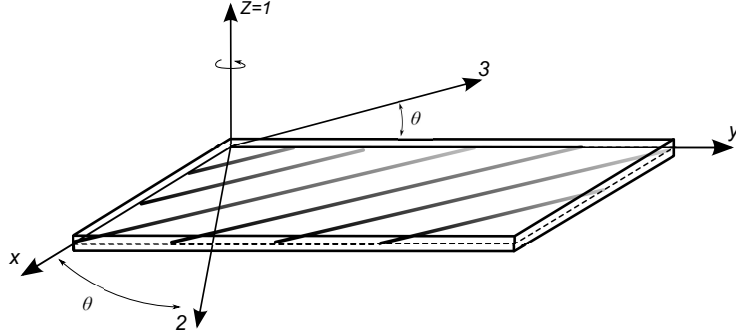


Figure 2: Material reference system.

\mathbf{C} is a symmetric matrix, then $C_{ij} = C_{ji}$. For this reason, it is composed by 21 independent elastic coefficients if a *anisotropic* material is considered. The *anisotropic* material has a different behavior over any direction considered. If the material has different proprieties along three perpendicular planes, it is a *orthotropic* material and the coefficients are reduced to 9 components.

The explicit forms of the matrix \mathbf{C} and of its components can be found in the books by Tsai [36] or Reddy [37].

As a consequence the transformation matrix \mathbf{T} is introduced:

$$\mathbf{T} = \begin{bmatrix} \cos^2\theta & \sin^2\theta & 0 & 0 & 0 & \sin 2\theta \\ \sin^2\theta & \cos^2\theta & 0 & 0 & 0 & -\sin 2\theta \\ 0 & 0 & 1 & 0 & 0 & 0 \\ 0 & 0 & 0 & \cos\theta & -\sin\theta & 0 \\ 0 & 0 & 0 & \sin\theta & \cos\theta & 0 \\ -\cos\theta\sin\theta & \cos\theta\sin\theta & 0 & 0 & 0 & \cos^2\theta - \sin^2\theta \end{bmatrix} \quad (6)$$

A *transformed material stiffness matrix* is introduced and it is expressed with the following form

$$\tilde{\mathbf{C}} = \mathbf{T}\mathbf{C}\mathbf{T}^T \quad (7)$$

This is the new stiffness matrix to be introduced in the Hooke's law.

$$\boldsymbol{\sigma} = \tilde{\mathbf{C}}\boldsymbol{\epsilon} \quad (8)$$

If the material has the same behavior in all directions, it is a *isotropic* material. This means that there is no preferential plane. Any chosen direction provides the same behavior. In this case, there is no need to define a material reference system and a rotation matrix. The performance of the material can be described with only one value of the Poisson ratio and of Young's modulus. These assumptions lead to have

$$C_{11} = C_{22} = C_{33} \quad C_{12} = C_{13} = C_{23} \quad C_{44} = C_{55} = C_{66} \quad (9)$$

Cross-sectional kinematic approximation

In the framework of the Carrera Unified Formulation, the displacement field \mathbf{u} can be written as the product of two contributions: one over the cross-section and one along the beam axis. If a one-dimensional model is considered, the beam contribution is referred to the beam axis y . The other contribution is a function of x and z . The displacement field becomes:

$$\mathbf{u}(x, y, z) = F_\tau(x, z)\mathbf{u}_\tau(y), \quad \tau = 1, 2 \dots M, \quad (10)$$

where \mathbf{u}_τ is the displacement vector, F_τ represents a function expansion used to approximate the behavior of the beam cross-section. M is the number of the expansion terms. The present work uses the Lagrange polynomials to describe the beam cross-section with high-order elements. The use of the Lagrange polynomials allows any cross-sectional geometry to be considered and an accurate description of the physical domain to be achieved. In this way, we have an accurate description

of the physical surface of the problem. An example of the discretization of a cross-section using Lagrange elements is shown in fig.3. If a nine-point element (L9) is used over the cross-section, the formulation of the displacement becomes:

$$\begin{aligned} u_x &= F_1 u_{x_1} + F_2 u_{x_2} + F_3 u_{x_3} \dots + F_9 u_{x_9} \\ u_y &= F_1 u_{y_1} + F_2 u_{y_2} + F_3 u_{y_3} \dots + F_9 u_{y_9} \\ u_z &= F_1 u_{z_1} + F_2 u_{z_2} + F_3 u_{z_3} \dots + F_9 u_{z_9} \end{aligned} \quad (11)$$

where $u_{x_1} \dots u_{x_9}$ represent the components x of the displacement field of each node of the L9 element. The Lagrange Elements introduce as unknowns only translational displacements. Figure 3 shows two simple ways to describe a section where more L9 or L4 elements are used.

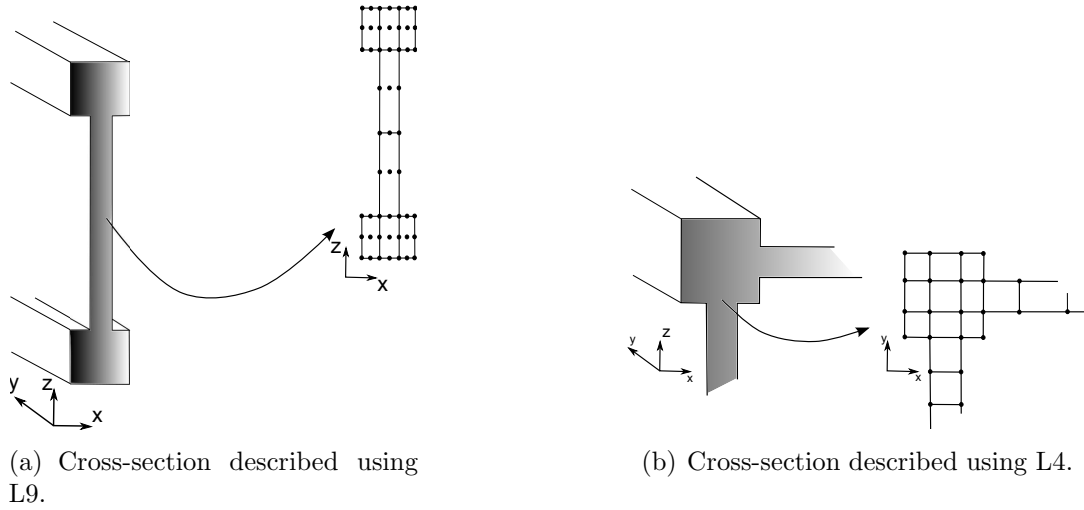


Figure 3: Example of cross-section discretization by Lagrange Elements.

Finite Element formulation

In order to solve the one-dimensional problem, the Finite Element model is used. The shape functions N_i are introduced to approximate the displacement over the beam axis (y). The vector \mathbf{u} can be written as

$$\mathbf{u}(x, y, z) = F_\tau(x, z) N_i(y) \mathbf{u}_{\tau i} \quad (12)$$

where $\mathbf{u}_{\tau i}$ is the nodal displacements vector.

The B3 elements (elements with three nodes) are adopted in this work and the index i indicates the i^{th} node of the beam element. The shape functions can be arbitrarily chosen but in this work the used shape function are reported in [25].

The governing equations can be achieved using the PVD (Principle of Virtual Displacements). In the static case, it is expressed as the equivalence between the work of the external loads (δL_{ext}) and the strain energy (δL_{int}). The term δ denotes the virtual variation.

$$\delta L_{int} = \delta L_{ext} \quad (13)$$

The strain energy can be written as a function of the stress and the virtual strain components:

$$\delta L_{int} = \int_V \delta \boldsymbol{\epsilon}^T \boldsymbol{\sigma} dV \quad (14)$$

$$\delta \boldsymbol{\epsilon} = \mathbf{b} F_s(x, z) N_j(y) \delta \mathbf{u}_{sj} \quad (15)$$

Introducing the Hooke's law and the geometrical relations, the internal work can be expressed as a function of the shape functions, the expansion used to describe the cross-section and the properties of the material.

$$\delta L_{int} = \delta \mathbf{u}_{sj}^T \int_V N_j(y) F_s(x, z) \mathbf{b}^T \tilde{\mathbf{C}} \mathbf{b} F_\tau(x, z) N_i(y) dV \mathbf{u}_{\tau i} \quad (16)$$

The stiffness matrix $\mathbf{k}^{ij\tau s}$ is represented by the integral. It is expressed in term of *fundamental nucleus* (FN). It is a 3×3 matrix and each its term has a fixed form, both for 1-D, 2-D and 3-D models. The nine terms of the FN can be found in [25].

The global stiffness matrix can be achieved varying the indexes i, j, τ and s . For a combination of i and j , each combination of τ (rows) and s (columns) is computed. To conclude the assembly procedure of the beam elements is performed.

The loading vector can be obtained from the external work. In the case of a concentrated load the external work can be written as

$$\delta L_{ext} = \delta \mathbf{u}^T P = \delta \mathbf{u}_{sj}^T N_{jP} F_{sP} \mathbf{P} \quad (17)$$

where N_{jP} and F_{sP} are the values of the function evaluated at the application point of the load \mathbf{P} . The term F_s is evaluated in (x_P, z_P) and N_j in (y_P) .

Rotation and Assembling Procedure

The present formulation allows each structure to be arbitrarily rotated and translated in the space. In this way, different components can be separately modeled and then, joined to obtain a complex structure composed by several elements. The rotation can be done through three rotation matrices around the three axes of the beam reference frame.

$$\begin{aligned}\Delta_x &= \begin{bmatrix} 1 & 0 & 0 \\ 0 & \cos(\theta) & \sin(\theta) \\ 0 & -\sin(\theta) & \cos(\theta) \end{bmatrix} & \Delta_y &= \begin{bmatrix} \cos(\phi) & 0 & \sin(\phi) \\ 0 & 1 & 0 \\ -\sin(\phi) & 0 & \cos(\phi) \end{bmatrix} \\ \Delta_z &= \begin{bmatrix} \cos(\xi) & -\sin(\xi) & 0 \\ \sin(\xi) & \cos(\xi) & 0 \\ 0 & 0 & 1 \end{bmatrix}\end{aligned}\quad (18)$$

$$\Delta = \Delta_z \Delta_y \Delta_x \quad (19)$$

In this way, a generic displacement \mathbf{u} in a local reference system, can be rotated from the local to the global reference system through the following formulation:

$$\mathbf{u}_G = \Delta \mathbf{u} \quad (20)$$

where \mathbf{u}_G is the displacement in the global reference system. The fundamental nucleus in a local reference system can be also referred to a global frame in this way:

$$\mathbf{k}_G^{ij\tau s} = \Delta^T \mathbf{k}^{ij\tau s} \Delta \quad (21)$$

In the present LE formulation, the structures can be joined very easily because, as said in the introduction, the unknowns are only displacements. The assembling is done just imposing the congruence of the displacements in the shared nodes. An example is represented in [4](#).

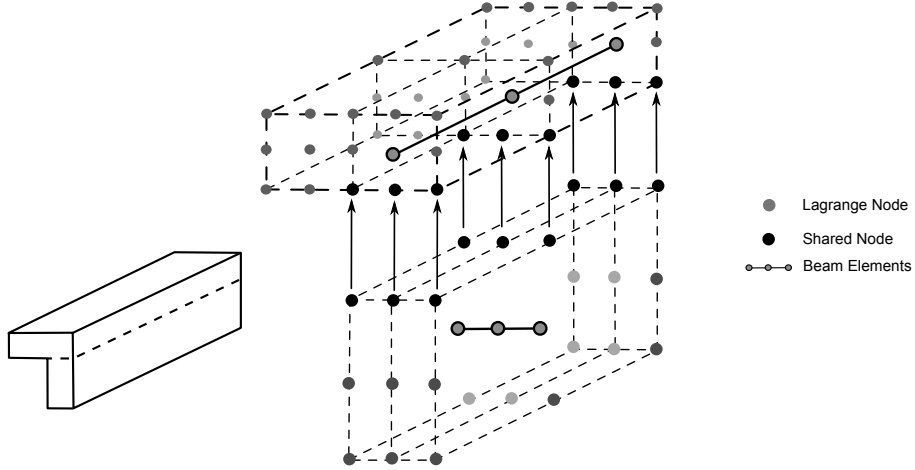


Figure 4: Example of structure assembling.

2.1 Tapered Structures modelling using the Component-wise approach.

As previously said, the *Component-wise approach* allows each component of a complex structure to be modeled with different beam elements, so with a different beam formulation. Through this approach, the analyses of tapered beams can be performed. To introduced the *Component-wise* concept the simple TWS shown in figure 5a in considered. The structure can be modeled with only one beam description using the *typical approach*. The largest length is used as beam axis and the cross-section includes the lateral face of the panel and the reinforcement cross-sections. A description with LE elements is represented in the picture. Using the *Component-wise approach* each component can be considered as an independent beam. In this case, shown in figure 5b, the two stiffeners are modeled with the beam elements along the reinforcement axes and the panel is modeled in a similar way using the same beam direction. The three different cross-section are shown in the picture. This approach provide the same model as in the first case but using a different modeling approach

Otherwise, the present model allows each component to be modeled with an arbitrary beam axis. For this reason, the panel can be modeled using the thickness direction as beam axis. This case is figured in 5c. Using a proper cross-sectional mesh of the panel, accurate results can be obtained with this approach. Assessment results are presented in [38]. The cross-sectional shape can be arbitrary assumed, that is, this approach ca be used to obtain tapered structures, as shown in Figure 5d.

Through the *Layer-wise approach*, when composite structures are considered, each ply of the laminate can be separately modeled. In this way, the accuracy of the results is improved and the complex stress behavior of the laminate can be described evaluating the values in critical areas such as the interlaminar zones. If the approach shown in 5b is considered, the cross-section, which is the thickness face of the panel, can be described in different ways through the Lagrange Elements. If a three-ply laminate is considered, the cross-section can be described as shown in figure 6a where L4 elements have been used to represent the cross-section. We can identify the three layers: the elements 1, 2, 3 defines the first layer, the elements 4, 5, 6 identifies the second one and the elements 7, 8, 9 represent the third layer. Using the present model, each Lagrange Element can have a different material and, if an orthotropic material is considered, each layer can have a different lamination. In this way, this approach allows to model each layer with exact proprieties without introducing, for example, an equivalent material.

If the approach represented in 5c is considered and the layer is homogeneous, the *Layer-wise approach* is applied using a different beam description for each layer. In this way, each ply is a different structure with a different material and

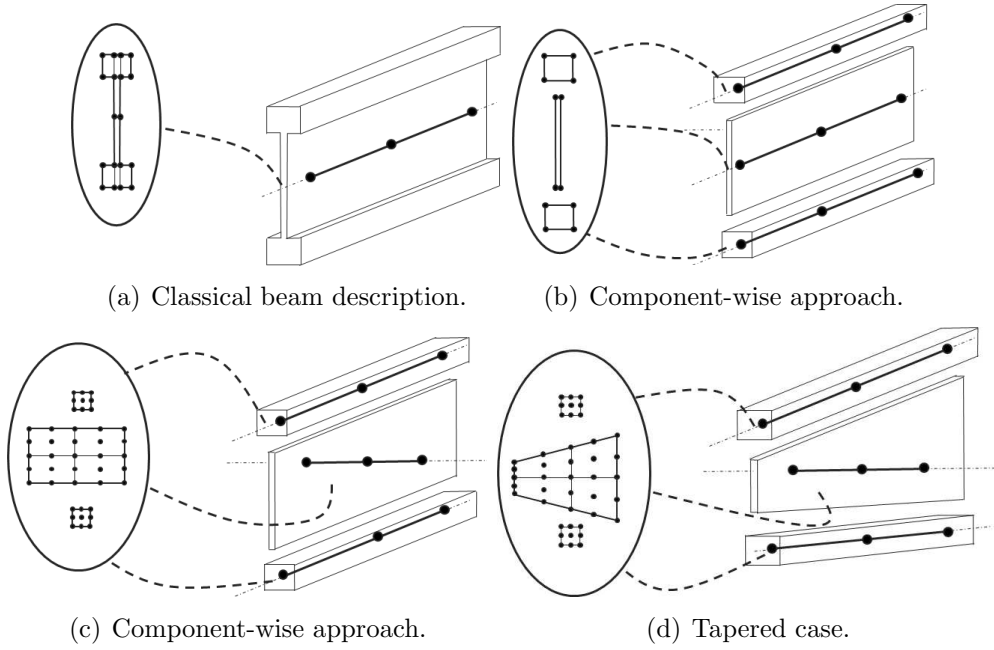


Figure 5: Examples of Component-wise approaches.

lamination. The case of a heterogeneous layer can be easily modeled modifying the proprieties of the Lagrange Elements over the involved areas. An example is a layer with a damaged area characterized by lower performances respect the rest of the ply.

3 Results

Different reinforced thin-walled structures will be presented in the following sections. Two materials are used. The first one is an Aluminium Alloy with the following proprieties : $E = 71.7 \text{ GPa}$, $\nu = 0.3$ and $\rho = 2.810 \text{ kg/m}^3$. This material has been used for the reinforcements. The second material is a *Carbon Fiber Reinforced Polymer CFRP* with these proprieties: $E_{LL} = 50 \text{ GPa}$, $E_{TT} = 10 \text{ GPa}$, $G = 5 \text{ GPa}$ and $\nu = 0.25$. The density is $\rho = 1.700 \text{ kg/m}^3$. E_{LL} identifies Young's modulus in the direction of the carbon fibers. The composite material is used for the panels of the structures. These components are 2-ply laminates with the lamination shown in fig.7. The results are compared with those obtained using two models built using the commercial code MSc/NASTRAN. These models are considered as valid reference solutions. The first model, called *Solid+Shell Model*, uses solid elements (*HEX8*) to model the stiffeners and shell elements (*QUAD4*) to model the composite panel. On the contrary, the second one, called *Beam+Shell*

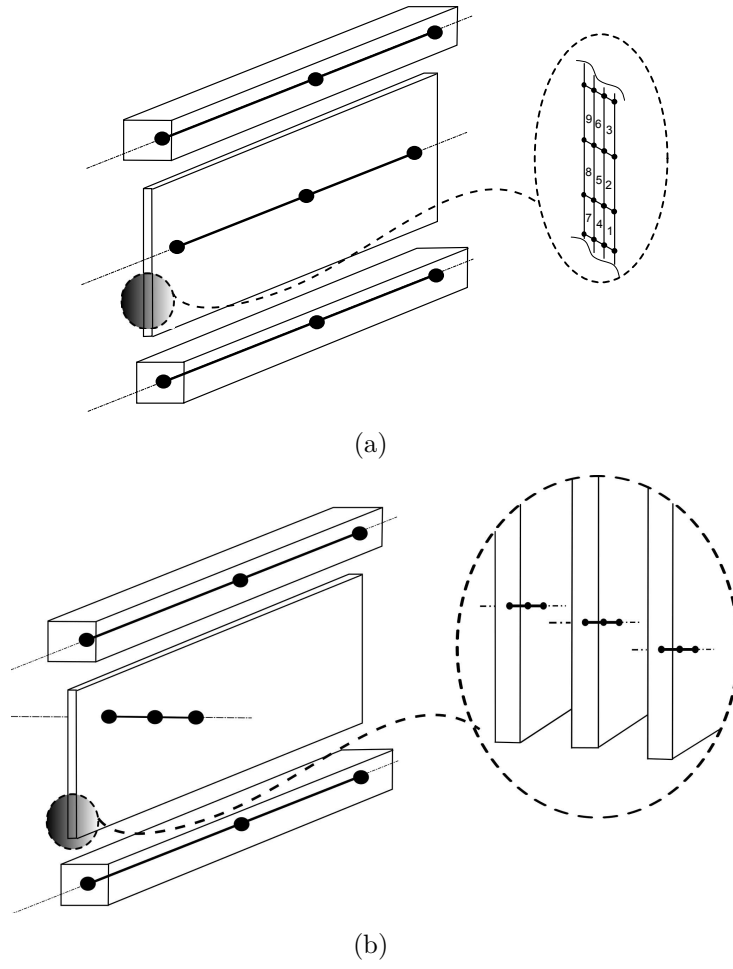


Figure 6: Examples of Layer-wise approaches in composite structures modeling.

Model, uses beam elements (*B2*) to model the stiffeners.

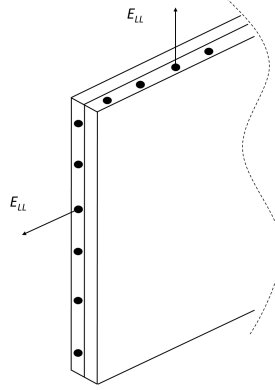


Figure 7: A two-ply laminate $0^\circ/90^\circ$.

4 Prismatic thin-walled composite beam.

The first structure analyzed is a reinforced thin-walled structure with a no-tapered shape. It is composed by two stiffeners and a rectangular panel. The two stiffeners and the panel are respectively made in the aluminum alloy and the composite material before introduced. The global structure has the following geometric characteristics: axial length $L = 1\text{ m}$, panel height $L = 0.2\text{ m}$, panel thickness $t = 0.002\text{ m}$, stiffness cross-section $a \times b = 0.02 \times 0.02\text{ m}$. One extremity is clamped and on the other side there is a punctual load. The force magnitude is $F = -50000\text{ N}$. The figure 8a shows the model considered.

The structure can be seen as the sum of three components: two stiffeners and the panel. Through the *Component-wise approach*, we used three different beam descriptions to model the components. The stiffeners are modeled in the *classical way* using the beam elements along the length of the reinforcement. 5 B3 elements are used. The cross-section of the reinforcement (the square surface) is described with Lagrange Expansion. The cross-section description is shown in fig. 8c. On the contrary, the thickness direction is taken as *beam axis* to model the panel. Considering the concept of the *Layer-wise approach*, a composite laminate can be modeled using different beam formulations for each layer. For each layer, one B3 element is used and the shape of the panel, the beam cross-section, is described using 20 L9 elements. This mesh has proved successful because of the results obtained in [38]. Figure 8b shows the descriptions used; the y axes identify the beam axes.

Table 3 shows the displacement results of the points a and b . The points are figured in 8d. The values are good compared to those obtained from the

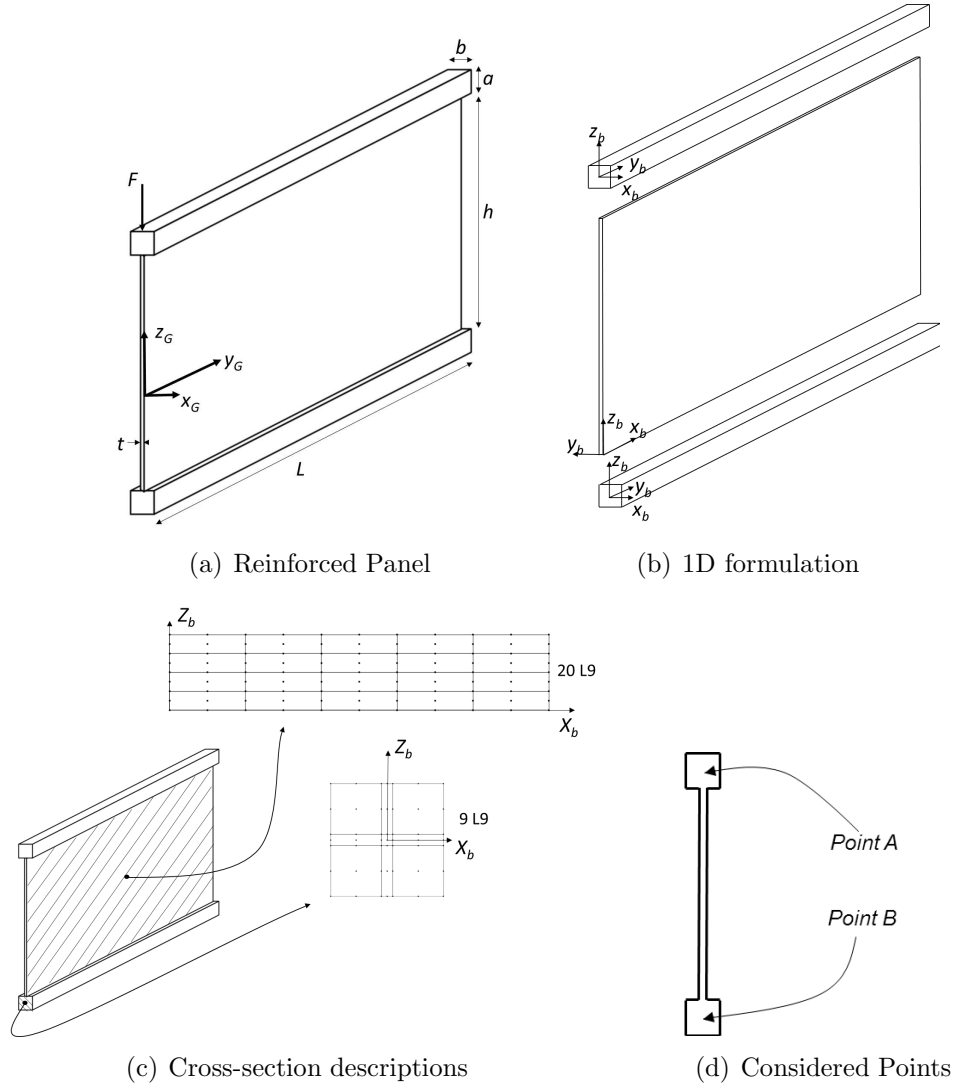


Figure 8: Rectangular case.

Solid+Shell model. The reported errors are respect the *Solid+Shell model*. The present model has about one-third of DOFs compared to the degree used by the *Solid+Shell Model*.

	DOF	w_a	w_b
Solid+Shell Model	14940	-4.219	-4.487
Beam+Shell Model	6960	-4.367	-4.671
Present Model	4521	-4.179	-4.360
%Err Solid+Shell	-68.78%	-0.95%	-2.83%

Table 1: Displacements w [$m \times 10^{-2}$] of the points a and b .

Table 2 shows the values of τ_{xz} in few points over the height of the panel. The results are compared to those obtained from the *Nastran Solid+Shell Model*. Figure 9b shows the distribution of the shear stress in the inter-laminal area over the length of the panel at $z = h/2$ and

z [m]	Nastran Solid+Shell Model	Present Model
0.100	-1.068	-1.064
0.075	-1.103*	-1.097
0.050	-1.138	-1.134
0.025	-1.162*	-1.154
0.000	-1.174	-1.170
-0.025	-1.172*	-1.163
-0.050	-1.157	-1.153
-0.075	-1.127*	-1.118
-0.100	-1.094	-1.082

*is obtained by the mean of the values around the point chosen.

Table 2: Rectangular case: in plane shear stress τ_{xz} [$Pa \times 10^8$]

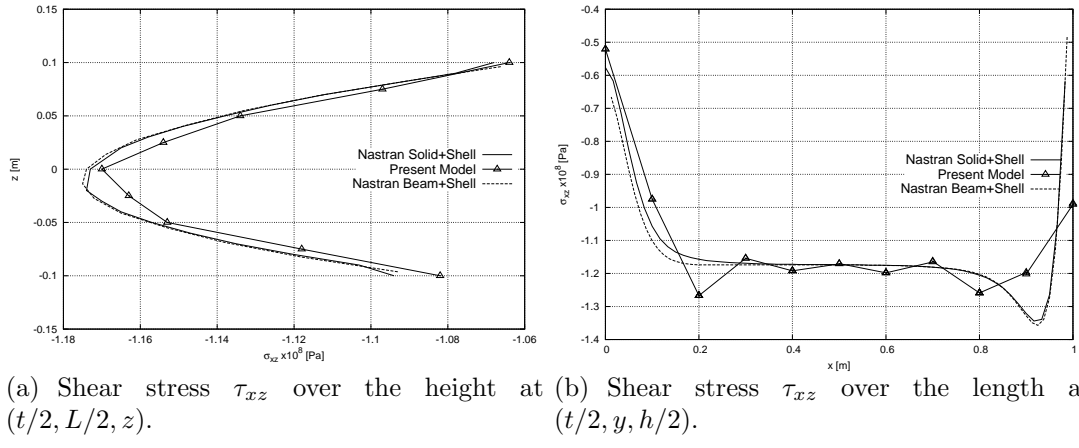


Figure 9: Shear stress behaviours.

5 Tapered thin-walled composite beam.

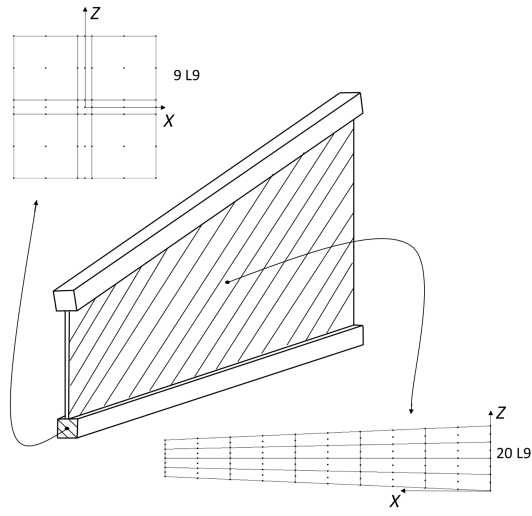
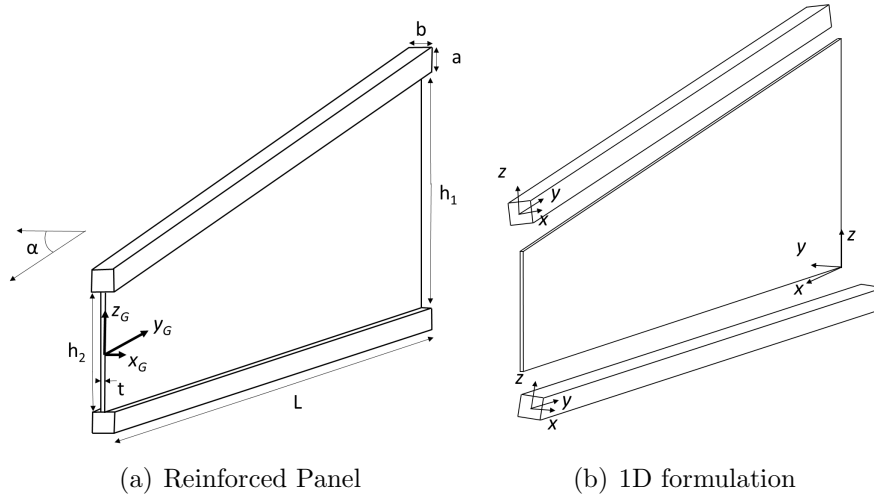
In this section a tapered thin-walled reinforced beam is considered. The geometry of the structure is shown in Figure 10. The layers of the laminate are always described with only one B3 element along the thickness for each layer. In this case, the cross-section geometry has been changed in order to provide a tapered shape. The cross-sectional discretization of the panel is shown in Figure 10c, can be achieved. Using the *Component-Wise approach* the tapered geometry can be described without the need of geometrical approximations as in the case of the stepped models. The reinforcements are described with five B3 elements over the length of the components. The cross-section description is the same used in the previous case. The stiffeners are rotated with an angle α to be connected to the panel. The geometrical data are shown in 10a and they have the following values: stiffeners length $L = 1\text{ m}$, the bigger height of the panel $h_1 = 0.2\text{ m}$, the other one is achieved by rotating the stiffener with an angle of $\alpha = 2.5\text{ deg}$. The value is $h_2 = 0.1128\text{ m}$. The panel thickness and the cross-section of the stiffener are the same the previous case. The applied force has a magnitude of $F = -50000\text{ N}$. The stiffeners are always made of aluminum alloy and the panel is a CFRP two-ply laminate.

Table ?? shows the displacement values of the two points before introduced. The results are very good and they are very close to those obtained by the model *Solid+Shell model*. In this case, the DOF's of the Nastran model have been increased to have better reference results. The present model provides low errors in each considered nodes.

	DOF	w_a	w_b
Solid+Shell Model	21860	-4.586	-4.409
Beam+Shell Model	15700	-4.823	-4.599
Present Model	4521	-4.535	-4.413
%Err Solid+Shell	-79.32%	-1.11%	0.09%

Table 3: Displacements w [$m \times 10^{-2}$] of the points a and b .

Table 4 shows the values of the shear stress in few points at $y = L/2$ between the two layers. The table compares the results of the present model with those obtained from the *Solid+Shell model*. On the maximum value at $z = 0$, the current model provides an error of only 0.2% using DOFs four times less respect the Nastran DOFs.



(c) Cross-section descriptions

Figure 10: Tapered case.

z [m]	Solid+Shell Model	Present Model
0.0782	-1.059	-1.048
0.0587	-1.074	-1.069
0.0391	-1.092	-1.093
0.0196	-1.103	-1.099
0.000	-1.107	-1.105
-0.0196	-1.105	-1.099
-0.0391	-1.095	-1.084
-0.0587	-1.077	-1.065
-0.0782	-1.062	-1.048
DOF	14940	4521

Table 4: Tapered case: in plane shear stress τ_{xz} [$Pa \times 10^8$].

Figure 11 shows the behaviour of the shear stress. The 11a represents the stress over the height of the panel at $y = L/2$. The dashed line represents the *Beam+Shell model* results. The figure 11b shows the effect of the tapered shape on the shear stress results. The values increase with the height reduction of the panel.

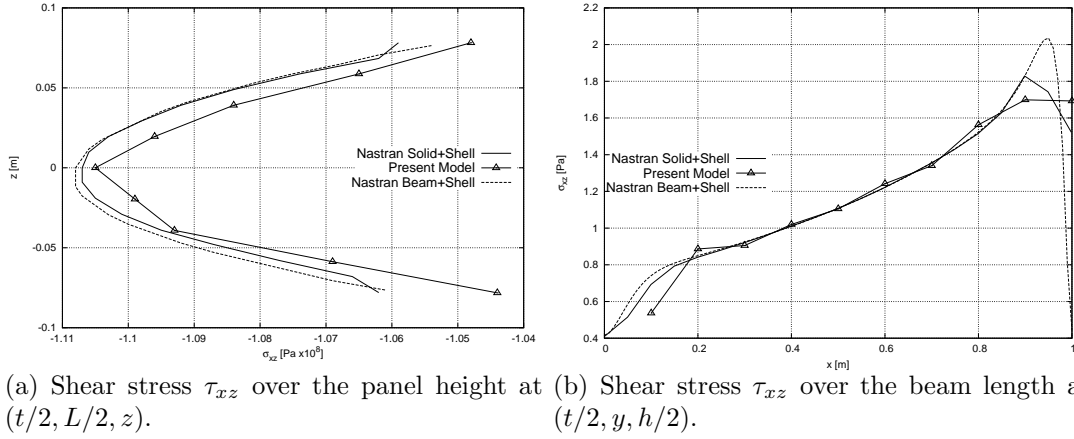


Figure 11: Shear stress behaviours.

6 Tapered composite wing-box structure.

This section introduces the analysis of a composite wing box structure. Four stiffeners and four composite panels are modeled and rotated in the space to obtain a tapered box with a close cross-section. The geometry is shown in 12. The geometrical values are the same of the previous sections. In this case the following new characteristics are introduced: the width at the root is $r_1 = 0.6 \text{ m}$ and the width at the tip is $r_2 = 0.5218 \text{ m}$. The panels are always made of CRFP laminate and the stiffeners made of aluminum alloy. Figure 13a shows the lamination used in this case. The external layers have the fiber direction along the y_G direction and the internal ones have the fibers along the traversal direction. The root extremity is always clamped. In this case, there is a punctual force on the stiffener number 2 as shown in 13b.

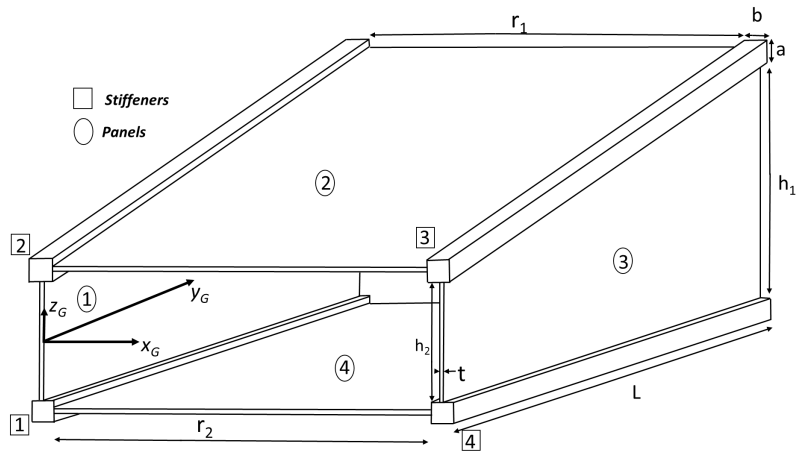
Figure 12 shows the beam descriptions used to model this structures. y identifies the beam axes. The stiffeners are modeled using five B3 elements along the reinforcement. The panels are modeled using the *Layer-wise approach*: each layer is modeled using one B3 element along the thickness. The same cross-sectional mesh of the previous cases have been used.

The displacements along the z -axis are evaluated in the four central points of the stiffeners. They are figured in 13b. The results from the present model are very accurate if compared with those from the reference solutions. They are very close to the *Solid+Shell model* and provide lower errors respect the values achieved from *Beam+Shell model*. The values are reported in the table 5.

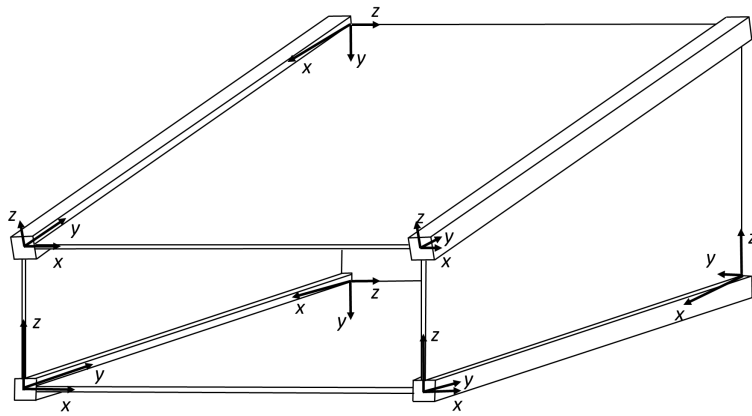
	DOFs	Point 1	Point 2	Point 3	Point 4
Present Model	11616	-3.726	-3.846	0.207	0.207
<i>Solid+Shell Model</i>	52480	-3.788	-3.965	0.213	0.213
<i>Beam+Shell Model</i>	48320	-3.966	-4.189	0.191	0.191
%Err Solid+Shell	-75.96%	-1.64%	-3%	-2.82%	-2.82%

Table 5: Displacements w [$m \times 10^{-2}$].

Figure 14 shows the behaviors of the obtained shear stress of the four panels which compose the structure. The figure a and c show the stresses concerning the vertical panels. The obtained results are accurate and very close to those from the Nastran code. The present model provides errors lower than 1%. On the panel number 3, some points provide a larger error. Figure b and d show the shear stress of the horizontal panels. All the three models show the same behaviors.



(a) Tapered Box.



(b) 1-D formulations.

Figure 12: Tapered Box.

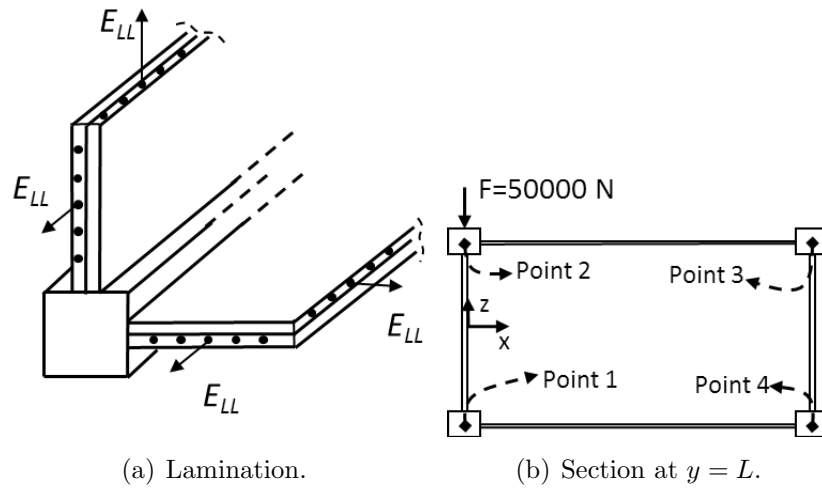
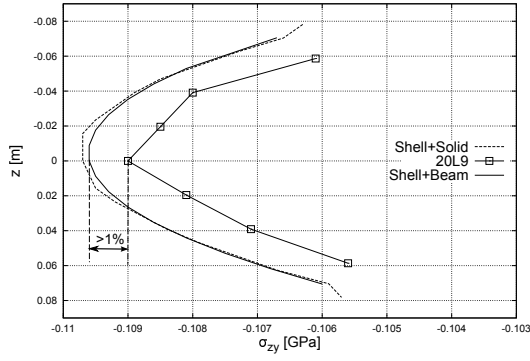
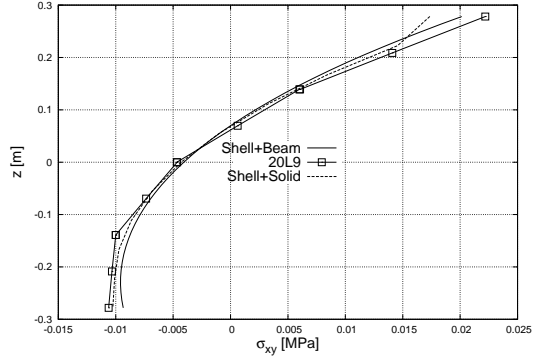


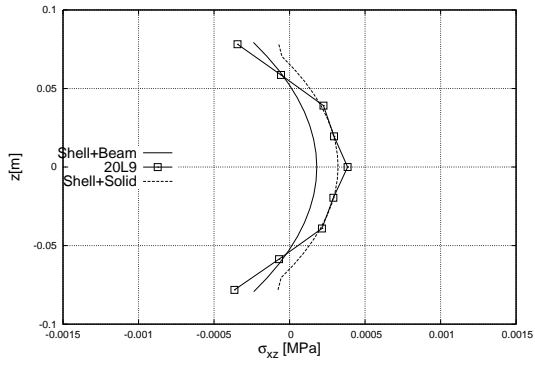
Figure 13: Lamination and load case.



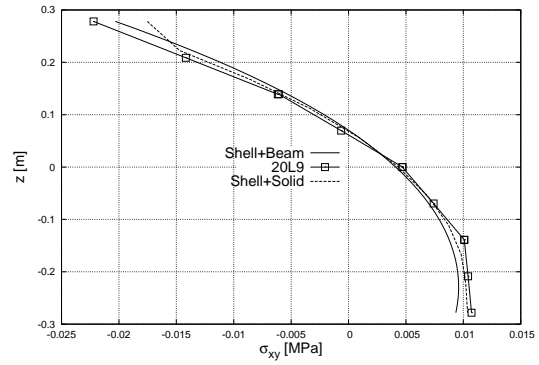
(a) Shear stress τ_{xz} of the panel 1 at $(t/2, L/2, z)$.



(b) Shear stress τ_{xz} of the panel 2 at $(t/2, L/2, z)$.



(c) Shear stress τ_{xz} of the panel 3 at $(t/2, L/2, z)$.



(d) Shear stress τ_{xz} of the panel 4 at $(t/2, L/2, z)$.

Figure 14: Shear stress behaviours.

7 Conclusions

This paper explores the capability of a refined one-dimensional model derived using the Carrera Unified Formulation in the analysis of thin-walled composite tapered structures. Different tapered structures, already analyzed by [38] in the isotropic case, has been taken into account. Through the *Layer-wise approach*, the composite material has been introduced. The panel has been described as a simple laminate and the behavior has been investigated. The displacement field has been verified too. The results confirm the capability of the present model to provide accurate results without high computational cost. The present model is able to describe with a high level of fidelity the geometries of the structures. In this way, the obtained results are very close to three-dimensional results. This advantage is due to the capability of this one-dimensional model to have a deformable cross-section. The results show values very close to those obtained from the typical models which are used in the analysis of these kind of structures. To conclude, the present model, thanks to the *Layer-wise approach*, can describe with a good accuracy the behaviour of a laminate which is different depending on the layers that compose it.

References

- [1] L. Euler. De curvis elasticis. Methodus inveniendi lineas curvas maximi minimive proprietate gaudentes, sive solutio problematis iso-perimetrici lattissimo sensu accepti. 1744.
- [2] J. R. Banerjee and F. W. Williams. Exact bernoulli-euler static stiffness matrix for a range of tapered beam-columns. *International Journal for Numerical Methods in Engineering*, 23(9):1615–1628, 1986.
- [3] P. Cicala. *Sulle travi di altezza variabile*. Laboratorio di Aeronautica, Tipografia Vincenzo Bona, Turin, Italy, 1939.
- [4] S.P. Timoshenko and J.N. Goodier. *Theory of elasticity*. McGraw-Hill, 1970.
- [5] Ji Yao Shen, Elias G. AbuSaba, William M. McGinley, Jr. Lonnie Sharpe, and Jr. Lawrence W. Taylor. Continuous dynamic model for tapered beamlike structures. *Journal of Aerospace Engineering*, 7(4):435–445, 1994.
- [6] M.J. Argyris and S. Kesley. *Energy Theorems and Structural Analysis*. Butterworths Scientific Publ., London,, 1960.

- [7] M.J. Turner, R.W. Clough, H.C. Martin, and L.J. Topp. Stiffness and Deflection Analysis of Complex Structures. *Journal of the Aeronautical Sciences*, 23(9):805–823, sep 1956.
- [8] D.J. Just. Plane frameworks of tapering box and I-section. *Journal of the Structural Division*, 103(1):71–86, 1977.
- [9] H.L. Schreyer. Elementary theory in linearly tapered beams. *Journal of the Engineering Mechanics Division*, 104(3):515–527, 1978.
- [10] C.J. Brown. Approximate stiffness matrix for tapered beams. *Journal of Structural Engineering*, 110(12):3050–3055, 1984.
- [11] A. Tena-Colunga. Stiffness formulation for nonprismatic beam elements. *Journal of Structural Engineering*, 122(12):1484–1489, 1996.
- [12] E.F. Bruhn. *Analysis and design of flight vehicle structures*. Tri-State Offset Company, 1973.
- [13] E. Carrera. *Fondamenti sul Calcolo di Strutture a Guscio Rinforzato per Veicoli Aerospaziali*. Levrotto & Bella, Turin, Italy, 2011.
- [14] S.U. Bescoter. A theory of torsion bending for multicell beams. *Journal of Applied Mechanics*, 53:25–34, 1954.
- [15] V.Z. Vlasov. *Thin walled elastic beams*. 1961.
- [16] P. Waldron. Sectorial properties of straight thin-walled beams. *Computers & Structures*, 24(1):147 – 156, 1986.
- [17] W. Yu, L. Liao, D.H. Hodges, and V.V. Volovoi. Theory of initially twisted, composite, thin-walled beams. *Thin-Walled Structures*, 43(8):1296 – 1311, 2005.
- [18] D.H. Hodges, A. Rajagopal, J.C. Ho, and W. Yu. Stress and strain recovery for the in-plane deformation of an isotropic tapered strip-beam. *Journal of Mechanics of Materials and Structures*, 5(6):963 – 975, 2010.
- [19] D.H. Hodges, A. Rajagopal, and W. Yu. The effect of taper on section constants for in-plane deformation of an isotropic strip. *Journal of Mechanics of Materials and Structures*, 5(6):963 – 975, 2010.
- [20] Y.Y. Kim and J.H. Kim. Thin-walled closed box beam element for static and dynamic analysis. *International Journal for Numerical Methods in Engineering*, 45(4):473–490, 1999.

- [21] D. Shin, S. Choi, G.W. Jang, and Y.Y. Kim. Finite element beam analysis of tapered thin-walled box beams. *Thin-Walled Structures*, 102:205 – 214, 2016.
- [22] E. Carrera. Theories and finite elements for multilayered plates and shells: A unified compact formulation with numerical assessment and benchmarking. *Archives of Computational Methods in Engineering*, 10(3):215–296, 2003.
- [23] E. Carrera, G. Giunta, P. Nali, and M. Petrolo. Refined Beam Elements With Arbitrary Cross-Section Geometries. *Comput. Struct.*, 88(5–6):283–293, 2010.
- [24] E. Carrera and M. Petrolo. Refined Beam Elements With Only Displacement Variables and Plate/Shell Capabilities. *Meccanica*, 47(3):537–556, 2012.
- [25] E. Carrera, M. Cinefra, M. Petrolo, and E. Zappino. *Finite Element Analysis of Structures Through Unified Formulation*. John Wiley & Sons, 2014.
- [26] E. Carrera, A. Pagani, and M. Petrolo. Classical, Refined and Component-wise Theories for Static Analysis of Reinforced-Shell Wing Structures. *AIAA Journal*, 51(5):1255–1268, 2013.
- [27] E. Carrera, A. Pagani, and M. Petrolo. Component-wise Method Applied to Vibration of Wing Structures. *Journal of Applied Mechanics*, 80(4):41012–41015, 2013.
- [28] E. Carrera and E. Zappino. Carrera Unified Formulation for Free-Vibration Analysis of Aircraft Structures. *AIAA Journal*, 54(1):280–292, jul 2015.
- [29] E. Carrera. The effects of shear deformation and curvature on buckling and vibrations of cross-ply laminated composite shells. *Journal of Sound and Vibration*, 150(3):405–433, 1991.
- [30] E. Carrera. c^0 reissner-mindlin multilayered plate elements including zig-zag and interlaminar stress continuity. *International Journal for Numerical Methods in Engineering*, 39:1797–1820, 1996.
- [31] E. Carrera. C_z^0 requirements-models for the two dimensional analysis of multilayered structures. *Composite Structures*, 37(3/4):373–383, 1997.
- [32] Filippi M. Carrera E. and Zappino E.. Laminated beam analysis by polynomial, trigonometric, exponential and zig-zag theories. *European Journal of Mechanics A/Solids*, 41:58–69, 2013.
- [33] Filippi M. Carrera E. and Zappino E.. Free vibration analysis of laminated beam by polynomial, trigonometric, exponential and zig-zag theories. *Journal of Composite Materials*, 48(19):2299–2316, 2014.

- [34] Petrolo M. Valvano S. Carrera E.. Filippi, M. Analysis of laminated composites and sandwich structures by trigonometric,exponential and miscellaneous polynomials and a mitc9 plate element. *Composite Structures*, 150:103–114, 2016.
- [35] Filippi M. and Carrera E.. Bending and vibrations analyses of laminated beams by using a zig-zag-layer-wise theory. *Composites Part B: Engineering*, 98:269–280, 2016.
- [36] S.W. Tsai. *Composites Design*. Dayton, Think Composites, 4th edition, 1988.
- [37] J.N. Reddy. *Mechanics of laminated composite plates and shells. Theory and Analysis*. CRC Press, 2nd edition, 2004.
- [38] Zappino E. Viglietti A. Carrera, E. The analysis of tapered structures using a component-wise approach based on refined one-dimensional models (submitted).